Journal of Cancer Research and Clinical Oncology (2024) 150:456
https://doi.org/10.1007/s00432-024-05938-5

RESEARCH

SCYL1-mediated regulation of the mTORC1 signaling pathway inhibits autophagy and promotes gastric cancer metastasis

Zihao Zhao[1,2,3] · Jinlong Liu[1,4] · Xian Gao[1,2,3] · Zhuzheng Chen[1,2,3] · Yilin Hu[1,2,3] · Junjie Chen[2,3] · Weijie Zang[1,2,3] · Wanjiang Xue[1,2,3]

Received: 16 July 2024 / Accepted: 2 September 2024 / Published online: 12 October 2024

Abstract

Background The SCY1-like (SCYL) family has been reported to be closely related to cancer metastasis, but it has not been reported in gastric cancer (GC), and its specific mechanism is not clear.

Methods We utilized databases like Deepmap, TCGA, and GEO to identify SCYL1's role in GC. Clinical samples were analyzed for SCYL1 expression and its correlation with patient prognosis. In vitro and in vivo experiments were conducted to assess SCYL1's function in GC cell migration, invasion, and autophagy.

Results SCYL1 showed an increased expression in GC tissues, which correlated with a negative prognosis. In vitro experiments demonstrated that SCYL1 promotes GC cell migration and invasion and inhibits autophagy. GSEA indicated an inverse relationship between SCYL1 and autophagy, while a direct relationship was observed with the mTORC1 signaling pathway. Knockdown of SCYL1 enhanced autophagy, while activation of mTORC1 reversed this effect.

Conclusions SCYL1 is a significant contributor to GC progression, promoting metastasis by activating the mTORC1 signaling pathway and inhibiting autophagy. These findings suggest SCYL1 as a potential therapeutic target for GC treatment.

Keywords SCYL1 · Gastric cancer · Metastasis · mTORC1 · Autophagy

Introduction

Gastric cancer (GC) ranks among the most common and deadliest types of cancer worldwide. Global cancer statistics indicate that the incidence and mortality rates of GC are significantly high, contributing to the global cancer burden (Sung et al. 2020). Even with the progress in early detection and therapeutic approaches in recent years, the five-year survival rate for GC patients is still under 30%, with some regions reporting even lower percentages. Postoperative recurrence is a major cause of poor prognosis in GC patients, with approximately 60% experiencing varying degrees of recurrence after surgery (Thrift and El-Serag 2020). This high recurrence rate underscores the urgent need for a deeper understanding of the biology of GC metastasis and the development of new therapeutic strategies to improve long-term patient survival.

The SCY1-like (SCYL) family comprises a group of proteins associated with intracellular transport, cell cycle regulation, and signal transduction (Yan et al. 2010). This family includes at least three known members: SCYL1, SCYL2, and SCYL3, all of which possess kinase domains and HEAT repeat sequences (Pelletier 2016). While the specific roles of their kinase activities in biological functions are not fully understood, they play significant roles in various intracellular processes. The association of the SCYL family with cancer metastasis has been confirmed in multiple studies. For instance, SCYL3 promotes the metastasis of hepatocellular

Zihao Zhao, Jinlong Liu and Xian Gao contributed equally to this work.

✉ Wanjiang Xue
xuewanjiang@ntu.edu.cn

Weijie Zang
zangweijie@stmail.ntu.edu.cn

1 Department of Gastrointestinal Surgery, Affiliated Hospital of Nantong University, Medical School of Nantong University, Nantong 226001, China

2 Research Center of Clinical Medicine, Affiliated Hospital of Nantong University, Nantong 226001, China

3 Nantong Key Laboratory of Gastrointestinal Oncology, Nantong 226001, China

4 Qidong People's Hospital, Nantong 226001, China

carcinoma by physically binding and regulating the stability and transactivating activity of ROCK2, leading to increased formation of actin stress fibers and focal adhesions (Lei et al. 2023). In addition, the STP axis, including SCYL1, promotes the metastasis of triple-negative breast cancer by degrading the REST tumor suppressor (Karlin et al. 2014). These findings reveal the potential functions of SCYL family members in cell dynamics and cancer metastasis, providing a foundation for further research.

Autophagy is a cellular degradation process that plays a complex role in cancer metastasis (Hou et al. 2020). Although autophagy typically helps cancer cells adapt to harsh environments, studies have shown that it might also suppress metastasis in certain cases (Tang et al. 2021). For instance, research indicates that inhibiting autophagy in breast cancer models slows tumor growth but unexpectedly promotes lung metastasis, suggesting a critical role for autophagy in limiting tumor invasiveness and spread (Marsh and Debnath 2020). The mTORC1 pathway is central to autophagy regulation, and its dysregulation in cancer may lead to persistent autophagy suppression, aiding cancer cell survival and metastasis (Debnath et al. 2023; Chen et al. 2021). Hence, investigating the interaction between mTORC1 and autophagy in cancer metastasis can enhance our understanding of how these processes drive tumor progression and help identify new therapeutic targets to curb cancer dissemination.

In this research, SCYL1 was pinpointed as a key factor in GC progression, confirmed by clinical data. Experiments showed SCYL1 boosts GC cell migration and invasion, relating to mTORC1 signaling and autophagy, offering insights for GC treatment.

Materials and methods

Clinical samples

A total of 110 paired specimens, comprising GC tissues and matched non-cancerous adjacent tissues, were collected by the Department of General Surgery at the Affiliated Hospital of Nantong University, China, from 2010 to 2011. The clinical data of GC patients are detailed in Table 1. Follow-up was conducted until August 2015, with a median duration of 38.4 months (range: 1.5 to 66.4 months). Histological diagnosis of GC was independently verified by two pathologists. All patients were treatment-naive with respect

Table 1 Relationships between SCYL1 expression and clinicopathological characteristics of GC patients (*P < 0.05)

Clinicopathological parameter	SCYL1 level		Total	*P* value
	High (n = 69)	Low(n = 41)		
Gender				
Male	44 (66.7%)	22 (33.3%)	66	0.295
Female	25 (56.8%)	19 (43.2%)	44	
Age (years)				
≤ 60	38 (72.7%)	15 (27.3%)	53	0.061
> 60	31 (54.4%)	26 (45.6%)	57	
Tumor differentiation				
Well	33 (55.9%)	27 (44.1%)	60	0.066
Moderate/Poor	36 (70.6%)	14 (29.4%)	50	
Tumor diameter (cm)				
≥ 5	32 (69.6%)	14 (30.4%)	46	0.209
< 5	37 (57.8%)	27 (42.2%)	64	
Tumor location				
Up	31 (72.1%)	12 (27.9%)	43	0.104
Middle/Down	38 (56.7%)	29 (43.3%)	67	
TNM stage				
I/II	35 (54.7%)	29 (45.3%)	64	0.040*
III	34 (73.9%)	12 (26.1%)	46	
Depth of invasion				
T1 + T2	40 (66.7%)	20 (33.3%)	60	0.349
T3 + T4	29 (58.0%)	21 (42.0%)	50	
Lymph node metastasis				
Positive	41 (71.9%)	16 (28.1%)	57	0.038*
Negative	28 (52.8%)	25 (47.2%)	53	

to radiotherapy, chemotherapy, or immunotherapy prior to their surgical resection.

Cell culture and in vitro functional experiments

Human gastric mucosal epithelial cells (GES-1) and a panel of GC cell lines (MKN-45, BGC-823, SGC-7901, AGS, HGC-27) were obtained from GeneChem (Shanghai, China). Cell cultivation was performed in RPMI-1640 medium enriched with 10% fetal bovine serum and antibiotics (100 U/mL of penicillin and streptomycin), procured from Clark (Shanghai, China) and Life Technologies (Shanghai, China), respectively. Wound healing assay and transwell assay were performed as previously described (Zang et al. 2022).

siRNA-mediated gene silencing

Specific siRNAs targeting SCYL1: si-SCYL1#1 (F:5′-GGCUACACCAGAUCGUGAATT-3′, R: 5′-UUCACGAUCUGGUGUAGCCTT-3′), si-SCYL1#2 (F:5′-CCGUGUCCAUCUUCGUCUATT-3′, R: 5′-UAGACGAAGAUGGACACGGTT-3′), si-SCYL1#3 (F:5′-GAGUAUCAGCAGAAGAUCATT-3′, R: 5′-UGAUCUUCUGCUGAUACUCTT-3′) and a non-targeting control were synthesized by Tsingke Biotech (Beijing, China). GC cells were transfected using jetPRIME (Suzhou, China), following the manufacturer's protocol (Liu et al. 2021).

Extraction of RNA and quantitative real-time PCR (qRT-PCR)

Total RNA was isolated from cells using standard protocols, and qRT-PCR was performed to quantify SCYL1: (F: 5′-TGACAGATGGGACGACGAAGA-3′, R: 5′-ATTTGGAGGATTTGTGGTCGG-3′) expression with specific primers, with GAPDH: (F: 5′-GGAAGCTTGTCATCAATGGAAATC-3′, R: 5′-TGATGACCCTTTTGGCTCCC-3′) serving as an internal control.

Western blot

Proteins were extracted from cell lines and subjected to Western blot analysis using antibodies specific to GAPDH (60,004-1-Ig), ULK1 (29,005-1-AP), p-ULK1 (80,218-1-RR), mTOR 66888-1-Ig) and p-mTOR (67,778-1-Ig) were purchased from Proteintech (Wuhan, China); SCYL1(A6735) from Abconal (Wuhan, China).

Autophagic flux determination

Autophagic flux was evaluated in SGC7901 cells transduced with GFP-mRFP-LC3 lentivirus (GeneChem, Shanghai, China). The specific operation is the same as before (Zang et al. 2022). Cells were treated with autophagy inhibitor 3-MA, fixed, and imaged to quantify autophagosome and autolysosome formation using fluorescence microscopy and the autophagosomes (yellow spots) and autolysomes (red spots) were counted using Image J software.

In vivo peritoneal metastasis assay in nude mice

Male athymic nude mice, four weeks old, were procured from the Animal Center of the Medical College of Nantong University and kept under controlled temperature and humidity conditions. All animal experiments were approved by the Animal Ethics Committee of Nantong University and conducted in accordance with the ARRIVE guidelines, the U.K. Animals (Scientific Procedures) Act, 1986, EU Directive 2010/63/EU for animal experiments, and the National Institutes of Health guide for the care and use of laboratory animals. Nude mice were utilized for the establishment of a peritoneal dissemination model, with injections of either siRNA-treated or control SGC7901 GC cells. Following a six-week period, mice were sacrificed, and metastatic nodules were quantified and subjected to immunohistochemistry (IHC) evaluation.

Tissue microarray (TMA) construction and IHC analysis

Tissue microarrays were assembled using a precision arraying instrument (Dako, Carpinteria, CA). The specific experimental procedure is as described earlier (Zang et al. 2021). All primary antibodies for IHC were shown below: SCYL1 (1:100), p-mTOR (1:200), LC3B (1:200). The IHC results were evaluated by two independent pathologists. Based on the expression level of SCYL1 in GC tissues compared to adjacent non-cancerous tissues, the samples were categorized into two distinct groups: those with high expression and those with low expression. The related scoring criteria refer to previous reports (Chen et al. 2022).

Microarray data acquisition and bioinformatics

The dependency of GC on SCYL family genes was interrogated using the DepMap portal (https://depmap.org/portal/), with expression analysis conducted on datasets from TCGA and GEO (GSE79973, GSE66229, GSE30727, GSE27342, GSE19826, GSE179252 and GSE13911). Survival analysis was performed using the Kaplan–Meier Plotter (www.kmplot.com), and GSEA (Gene Set Enrichment Analysis) generated angenerate an ordered list of all related genes based on their correlation with SCYL1 expression (Subramanian et al. 2005; Hu et al. 2024). The "c2.cp.all.v2022.1.Hs.symbols.gmt" and "h.all.

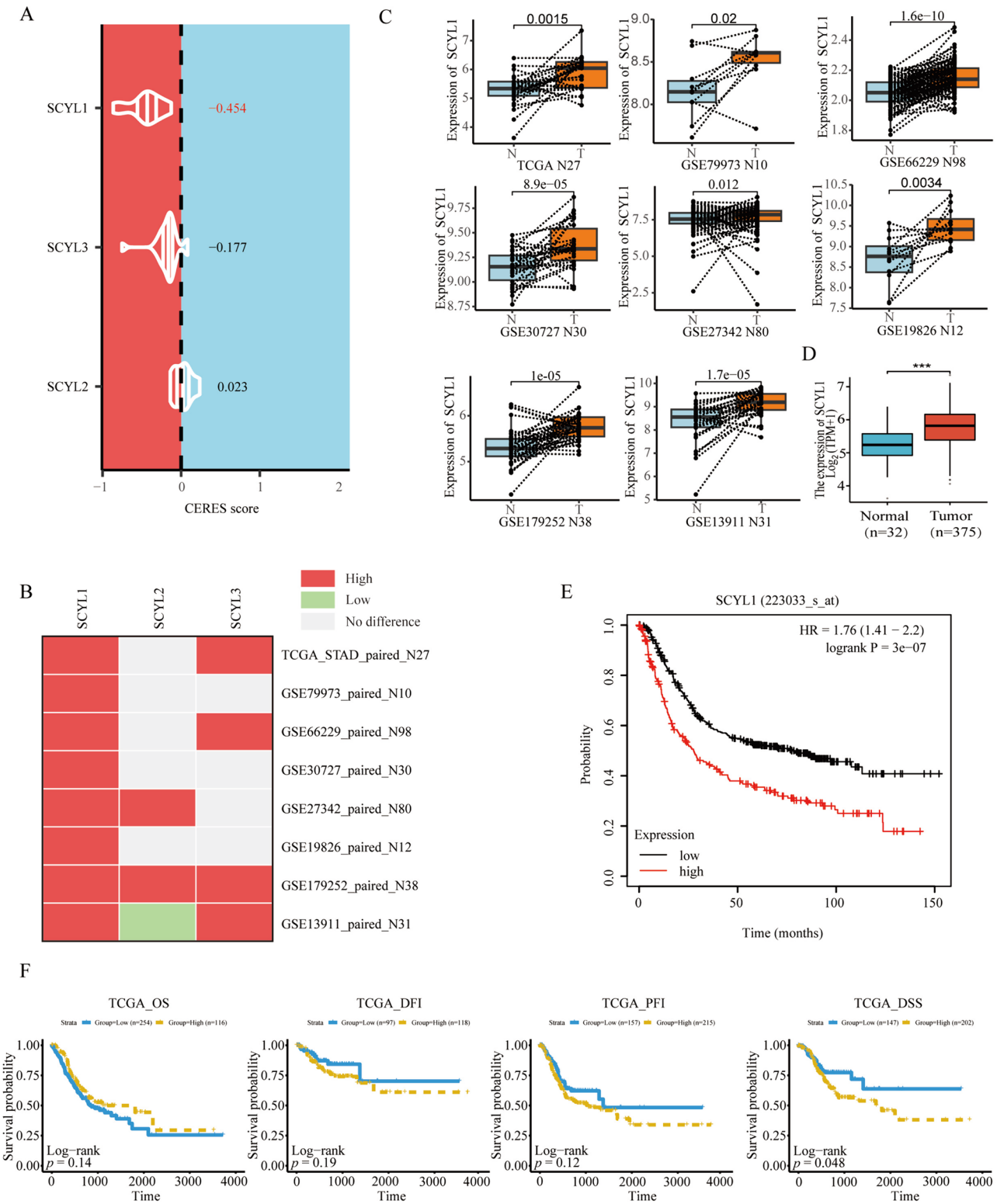

v7.5.1.symbols.gmt" were selected as reference gene sets. The data for single-cell sequencing is from the GEO database GSE163558, and cell annotation was performed using the "Seurat" R package (Jiang et al. 2022; Hao et al. 2021).

Statistical analysis

Quantitative data were presented as mean ± SD. Statistical analysis was performed using SPSS version 22, with survival outcomes analyzed via Kaplan–Meier and Cox

◂**Fig. 1** SCYL1 is predicted to be upregulated in GC tissues and associated with poor prognosis based on online databases. (**a**) Genome-wide CRISPR-Cas9 essentiality screening of SCYL family members in 20 gastric adenocarcinoma cell lines, yielding CERES scores. Original data were downloaded from DepMap. According to CERES scores, lower scores indicate higher cancer dependency on specific genes. (**b**, **c**) Expression of SCYL family members in paired GC tissues, data sourced from TCGA and GEO databases. Red indicates higher expression in GC, green indicates lower expression, and grey represents no significant difference. (**d**) Expression levels of SCYL1 in GC and normal tissues in all TCGA-STAD samples. (**e**) Relationship between SCYL1 expression levels and overall survival rates of GC patients in the Kaplan–Meier Plotter database. (**f**) In the TCGA database, the correlation of SCYL1 with OS (Overall Survival), DFI (Disease-Free Interval), PFI (Platinum-Free Interval) and DSS (Disease-Specific Survival)

regression methods (Liu et al. 2023). The significance of differences between experimental conditions was determined using the t-test, with a p-value threshold of < 0.05 for significance.

Results

SCYL1 is predicted to be upregulated in GC tissues and associated with poor prognosis based on online databases

In order to screen out SCYLs that are linked with GC, we first utilized the Deepmap database to screen for genes that significantly affect the progression of 20 types of gastric adenocarcinoma cells. We discovered that among SCYLs, the knockdown of SCYL1 showed the most prominent inhibitory effects on the functions of gastric adenocarcinoma cells. (Fig. 1a). Further, through analyzing 8 sets of paired GC tissue microarrays from TCGA and GEO databases (GSE79973, GSE6629, GSE30727, GSE27342, GSE19826, GSE179252, and GSE13911), we found that SCYL1 was highly expressed in all of them (Fig. 1b and Fig. 1c). Similarly, in the unpaired samples of TCGA-STAD, SCYL1 was also found to be highly expressed in GC tissues (Fig. 1d). According to the Kaplan–Meier Plotter online database, elevated SCYL1 expression was indicative of a negative prognosis (Fig. 1e). In the TCGA database, although there was no difference, high expression of SCYL1 predicted a poor prognosis in OS (Overall Survival), DFI (Disease-Free Interval), PFI (Platinum-Free Interval) and DSS (Disease-Specific Survival), with statistical differences observed in DSS ($P = 0.048$) (Fig. 1f). Based on the predictions from the aforementioned online databases, we chose SCYL1 for further study.

SCYL1 is significantly upregulated in clinical GC samples and is associated with poor prognosis

Building upon our previous findings, we further investigated the expression of SCYL1 in clinical samples. Initially, we examined the expression of SCYL1 in 20 pairs of GC tissues using qRT-PCR, which revealed an upregulation of SCYL1 in GC tissues (Fig. 2a). Subsequently, we analyzed the expression of SCYL1 in GC tissue microarrays via IHC and compared it with normal tissue samples ($n = 110$). A higher expression of SCYL1 was observed in 62.7% (69/110) of GC tissues compared to normal gastric tissues ($P < 0.01$; Fig. 2b). We then analyzed the correlation between various clinicopathological factors and the level of SCYL1 expression in 110 GC patients (Table 1). A positive correlation was found between SCYL1 expression and lymph node metastasis ($P = 0.038$) and TNM stage ($P = 0.040$). Moreover, multiple logistic regression analysis revealed a significant correlation between SCYL1 expression and lymph node metastasis ($P < 0.001$, odds ratio = 5.081, 95% confidence interval [CI]: 2.064–12.508). Furthermore, high SCYL1 expression in GC patients was significantly associated with reduced overall OS and DFS (Fig. 2c and d). Additionally, Cox multivariate analysis indicated that high expression of SCYL1 is an independent predictor of OS and DFS (Table 2). Collectively, our findings demonstrate a clear association between increased SCYL1 expression and GC progression and survival.

In vitro experiments show that SCYL1 promotes the migration and invasion of GC cells

Drawing from prior studies that highlight a strong association between SCYLs and cancer metastasis (Lei et al. 2023; Sun et al. 2022), and our clinical sample univariate and multivariate analyses showing that SCYL1 is closely related to lymphatic metastasis. Based on single-cell sequencing data, SCYL1 is significantly higher in metastatic tissues of GC compared to the primary site (Fig. 3a–c). Thus, we conducted related in vitro experiments to verify the impact of SCYL1 on GC metastasis. We found increased expression of SCYL1 in GC cell lines compared to the GES-1 cell line by qRT-PCR and WB (Fig. 3d–e). To examine if SCYL1 had an impact on the biological characteristics of GC cells, we transfected three si-SCYL1 fragments (si-SCYL1#1, si-SCYL1#2, and si-SCYL1#3) into SGC7901 cells. The effectiveness of this process was then assessed using qRT-PCR and WB, among them, si-SCYL1#1 has the highest knockdown efficiency (Fig. 3f–g). Following this, we conducted wound healing and transwell assays to determine if SCYL1 significantly influences GC migration and invasion. It was observed that a decrease in SCYL1 expression led to a reduction in the migratory capability of GC cells when compared to the NC groups (Fig. 3h–k).

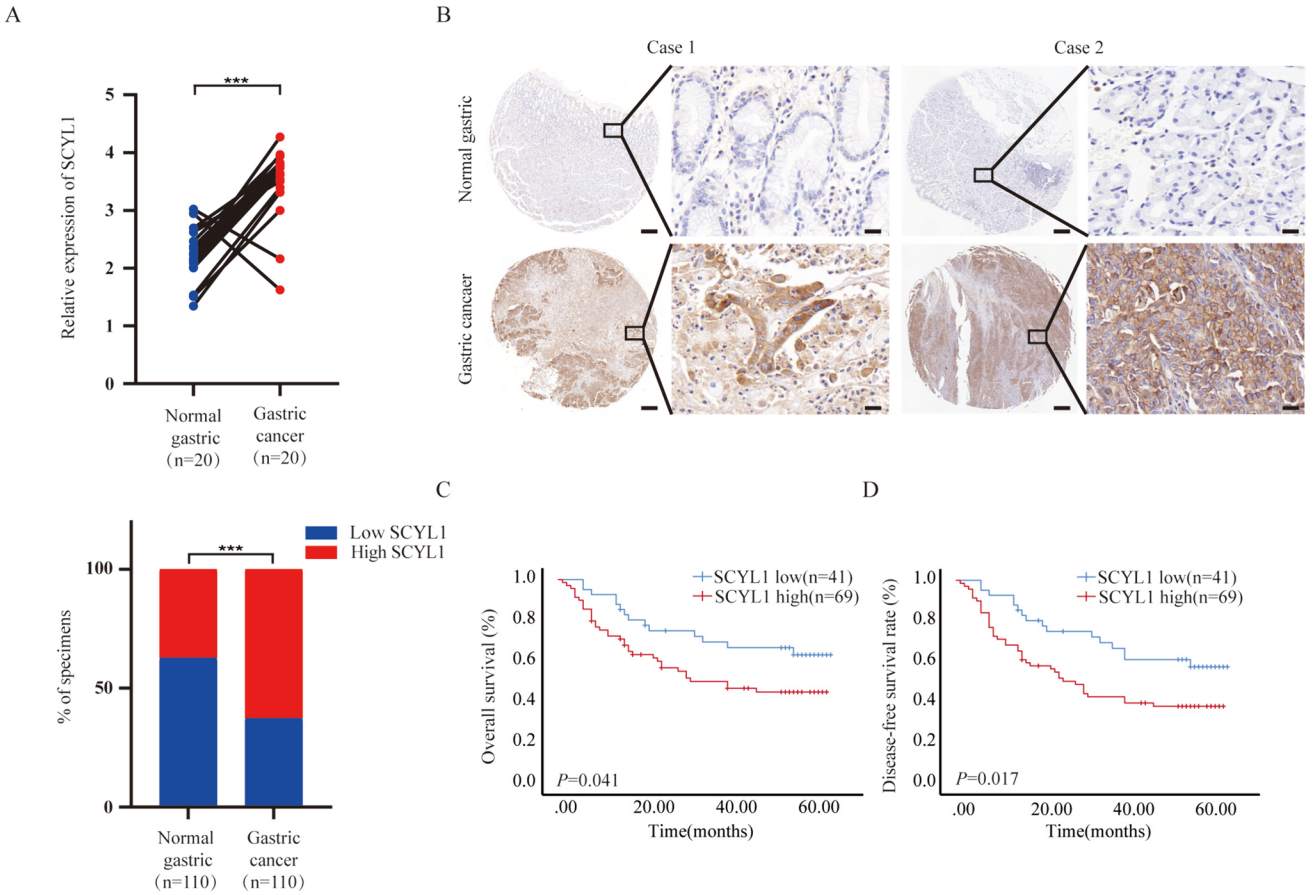

Fig. 2 SCYL1 is significantly upregulated in clinical GC samples and is associated with poor prognosis. (**a**) qRT-PCR analysis of SCYL1 expression levels in 20 pairs of fresh GC tissue samples. (**b**) Typical tissue microarray image analysis of SCYL1 expression in 110 patients. Scale bar, 50 μm. (**c**) Quantification of SCYL1 expression by immunohistochemistry analysis. (**d**) OS ($P=0.041$) and DFS ($P=0.017$) of GC patients related to SCYL1 expression by Kaplan–Meier survival curve analysis

SCYL1 inhibits autophagy in GC cells, promoting their migration and invasion

To further explore the mechanism by which SCYL1 affects the metastasis of GC, we divided TCGA-STAD samples into two groups based on the expression level of SCYL1 (Fig. 4a) and ranked the mRNA of the coding proteins from high to low according to $\log_2$FC for GSEA analysis (KEGG gene set). We found that SCYL1 was significantly negatively correlated with autophagy (Fig. 4b). Previous literature reported that inhibiting the autophagic degradation of GC cells could promote the migration, and invasion of GC cells (Aslan et al. 2019). Hence, we examined the effect of SCYL1 on autophagy by introducing the GFP-mRFP-LC3 lentivirus into GC cells SGC7901. Post-transfection of GFP-mRFP-LC3 lentivirus, there was an increase in the count of red puncta (autolysosomes) in si-SCYL1#1 GC cells, suggesting an enhancement in autophagic flux. An increase in yellow dots (autophagosomes) was observed when the autophagic flux was obstructed by 3-Methyladenine (an inhibitor of autophagosome/lysosomal fusion) (Fig. 4c and d). WB results corroborated that post si-SCYL1, there was a significant elevation in LC3 protein levels (Fig. 4e), implying that si-SCYL1 facilitated autophagy in GC cells. At the same time, wound healing and transwell assays proved that after autophagy was inhibited by 3-MA, the migration and invasion abilities of GC cells could be significantly restored (Fig. 4f–i).

SCYL1 inhibits autophagy in GC through activating the mTORC1 signaling pathway

In order to uncover the mechanism by which SCYL1 affects autophagy in GC cells, we conducted GSEA enrichment analysis based on the TCGA dataset. The results indicated that the expression of SCYL1 was positively correlated with the mTORC1 signaling pathway in GC tissues (Fig. 5a). Previous studies have demonstrated that the mTORC1 signaling pathway is involved in regulating cell growth, epithelial-mesenchymal transition (EMT), migration, and invasion in

Table 2 Univariate and multivariable analyses of OS and DFS in GC patients (*P < 0.05)

Variable	OS			DFS		
	Univariate analysis	Multivariable analysis		Univariate analysis	Multivariable analysis	
	P >|z|	*P* >|z|	HR (95% CI)	*P* >|z|	*P* >|z|	HR (95% CI)
Gender	0.245			0.900		
Male (n = 66) vs						
Female (n = 44)						
Age (years)	0.654			0.840		
≤ 60 (n = 53) vs						
> 60 (n = 57)						
Tumor differentiation	0.685			0.703		
Well (n = 60) vs						
Moderate/Poor(n = 50)						
Tumor diameter (cm)	0.875			0.975		
≥ 5 (n = 46) vs						
< 5 (n = 64)						
Tumor location	0.286			0.299		
Up (n = 43) vs						
Middle/Down (n = 67)						
TNM stage	0.258			0.125		
I/II (n = 64) vs						
III/IV (n = 46)						
Depth of invasion	0.041*	0.093		1.634(0.921–2.901)	0.059	
T1 + T2 (n = 60) vs						
T3 (n = 50)						
Lymph node metastasis	0.002*	< 0.001*	2.948(1.606–5.413)	0.005*	< 0.001*	2.761(1.602 ~ 4.760)
Negative (n = 57) vs						
Positive (n = 53)						
SCYL1 expression	0.046*	0.002*	2.781(1.463 ~ 5.286)	0.021*	0.001*	2.661(1.466 ~ 4.828)
Low (n = 41) vs						
High (n = 69)						

various cancers, as well as being capable of suppressing the autophagy levels in cancer cells (Maynard et al. 2020; Li et al. 2021). To verify the results of the GSEA, we employed Western blot to assess the expression of mTORC1-related effectors (mTOR and ULK1). As shown in Fig. 5b, the phosphorylation levels of mTOR and ULK1 in SGC7901 cells with SCYL1 knocked down were decreased compared to the NC group, indicating the suppression of the mTORC1 signaling pathway. In vitro experiments, we demonstrated that knocking down SCYL1 could significantly promote autophagy in GC cell, whereas the use of the mTORC1 activator MHY1485 noticeably suppressed the autophagy levels in GC cells (Figs. 5c–e).

SCYL1 promotes migration of GC cells in vivo

Then, we suppressed the expression of SCYL1 in the SGC7901 cell line and examined the influence of SCYL1 expression on GC metastasis using a peritoneal dissemination model in nude mice (Fig. 6a). The average number of macroscopic nodules in the si-SCYL1#1 group was significantly reduced compared to the CON group (Fig. 6b). And, the IHC results of peritoneal metastatic nodules showed that the expression of SCLY1 was positively correlated with p-mTOR, while negatively correlated with the autophagy marker LC3B (Fig. 6c). In summary, our findings reveal that SCYL1 promotes the metastasis of GC cells by activating the mTORC1 signaling pathway and inhibiting autophagy in GC (Fig. 6d).

Discussion

This study primarily focuses on the expression of the SCYL1 gene in GC tissues and its relationship with prognosis, aiming to delve into the role of SCYL1 in the progression of

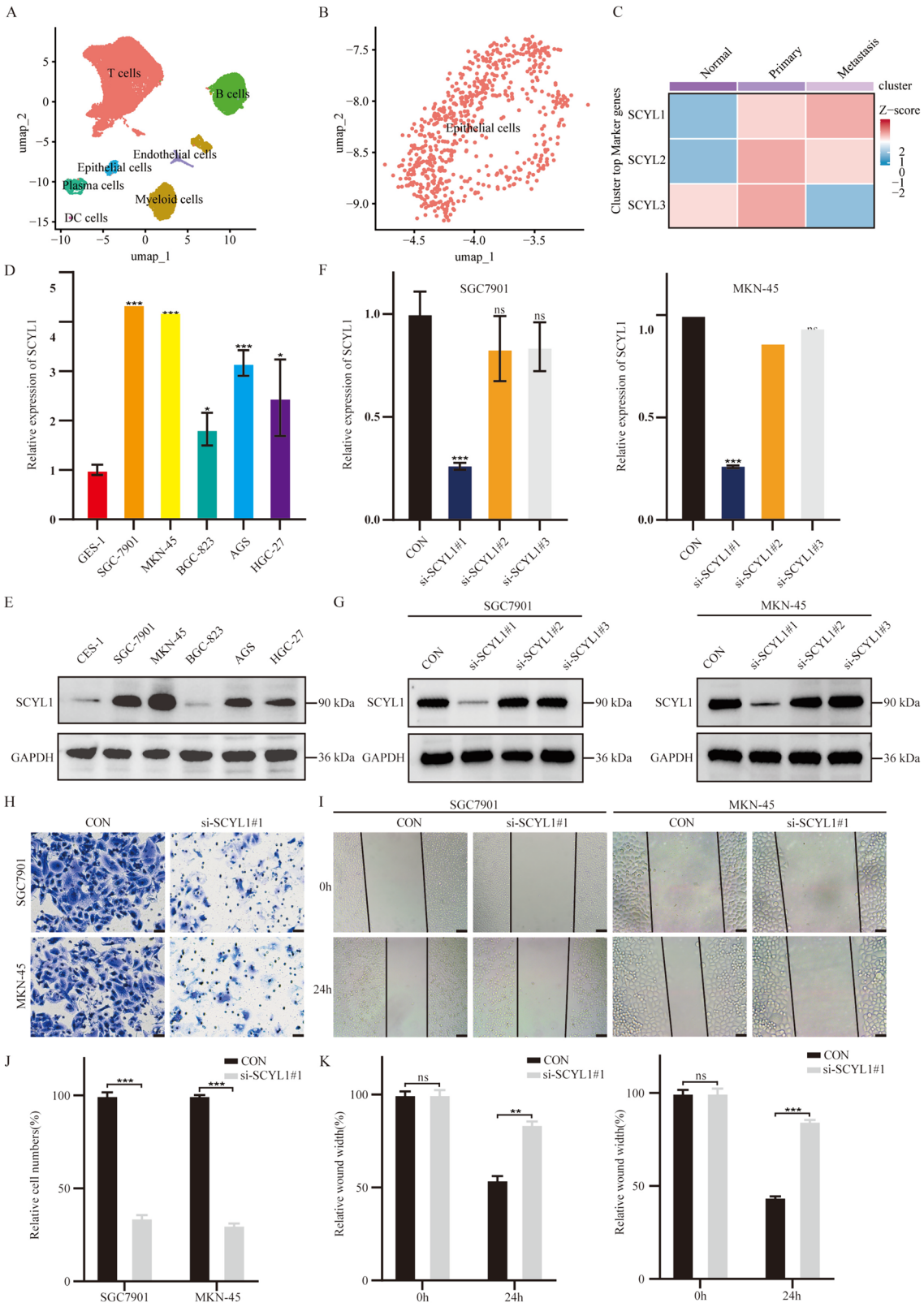
A
T cells
B cells
Endothelial cells
Epithelial cells
Plasma cells
Myeloid cells
DC cells
umap_1
umap_2
B
Epithelial cells
umap_1
umap_2
C
Normal
Primary
Metastasis
cluster
Z−score
SCYL1
SCYL2
SCYL3
Cluster top Marker genes
D
Relative expression of SCYL1
GES-1
SGC-7901
MKN-45
BGC-823
AGS
HGC-27
F
SGC7901
MKN-45
Relative expression of SCYL1
CON
si-SCYL1#1
si-SCYL1#2
si-SCYL1#3
ns
E
SCYL1
GAPDH
90 kDa
36 kDa
G
SGC7901
MKN-45
H
CON
si-SCYL1#1
SGC7901
MKN-45
I
0h
24h
J
Relative cell numbers(%)
K
Relative wound width(%)

◂**Fig. 3** In vitro experiments show that SCYL1 promotes the migration and invasion of GC cells. (**a**) The single-cell annotation plot for the GSE163558 chip. (**b**) Epithelial cells in the GSE163558 chip. (**c**) Expression of SCYLs in normal gastric tissue, primary GC tissue, and metastatic GC tissue. (**d**, **e**) qRT-PCR and WB analysis of SCYL1 mRNA expression levels in various GC cell lines and normal gastric mucosal epithelial cells. (**f**, **g**) qRT-PCR and WB analysis of siRNA knockdown efficiency of SCYL1 in GC cells. (**h**, **i**) Transwell and wound healing assays to assess the impact of si-SCYL1 on the migratory ability of GC cells SGC7901. (**j**, **k**) Quantification of transwell (**j**) and wound healing assays (**k**). Scale bar, 50 μm. (ns, $P > 0.05$; $^{**}P < 0.01$; $^{***}P < 0.001$)

GC and its underlying molecular mechanisms. Through predictive analysis using online databases and validation with clinical samples, we have discovered that SCYL1 expression is significantly upregulated in GC tissues and closely associated with lymph node metastasis, tumor invasion depth, and poor prognosis. Additionally, in vivo and in vitro experiments further confirm that SCYL1 facilitates the metastasis of GC. Mechanistically, SCYL1 promotes GC metastasis by activating the mTORC1 signaling pathway and inhibiting cellular autophagy. These findings provide a fresh viewpoint on the molecular pathology of GC and may offer novel targets for the diagnosis and treatment of the disease.

SCYL1, as an intracellular protein kinase and regulator, has garnered increasing attention for its role in neurodegenerative diseases and cancer progression in recent years (Hu et al. 2012). For instance, diseases of motor neurons caused by the deficiency of SCYL1 (Kuliyev et al. 2018). Despite this, research has found that SCYL1, which is overexpressed in breast cancer, has been linked to unfavorable clinical outcomes in patients. Notably, the use of shRNA to suppress SCYL1 has been shown to significantly inhibit the proliferation and migration of breast cancer cells (Sun et al. 2022). However, there is a severe lack of research in the area of GC. Our study bridges this gap by systematically revealing the expression pattern of SCYL1 in GC tissues and its correlation with prognosis, providing a new direction for research into the molecular mechanisms of GC.

mTORC1 is commonly associated with cancer (Ke et al. 2017). Numerous oncogenes are situated upstream of mTORC1, leading to the hyperactivation of the mTORC1 pathway in various cancers (Yang et al. 2017). Conversely, genes that inhibit mTORC1 signaling have been reported as tumor suppressors (Saxton and Sabatini 2017). Consistent with this notion, we have identified SCYL1 as a potential oncogenic factor that promotes GC cell metastasis through the positive regulation of mTORC1 signaling. This discovery may serve as a potential therapeutic strategy to inhibit GC metastasis.

Acknowledging the potential impact of these findings, we must also consider the study's limitations and avenues for future research. While these findings contribute to our understanding of GC progression, the scope of our analysis is constrained by factors such as a relatively small sample size and the use of existing bioinformatics databases and retrospective data analysis. These factors may limit the generalizability and interpretive power of our results. Secondly, SCYL family proteins are categorized as pseudokinases (Pelletier 2016), meaning they have kinase-like domains but are predicted to lack kinase activity due to changes in key catalytic residues. However, our study indicates that the downregulation of SCYL1 in GC inhibits the phosphorylation levels of mTORC1, suggesting that there may be other regulatory mechanisms involved, which warrants further investigation. Future research is required to validate our findings in larger, independent cohorts and to explore the mechanisms and clinical utility of SCYL1 in GC development through prospective studies.

Conclusion

Our research underscores the significant role of SCYL1 in the progression of GC and reveals its potential as a target for therapeutic intervention. SCYL1 is highly expressed in GC tissues and is significantly associated with poor survival outcomes in patients. Experiments both in vivo and in vitro have demonstrated its capability to enhance the migration and invasion of GC cells. Mechanistically, SCYL1 drives GC metastasis by inhibiting autophagy via activation of

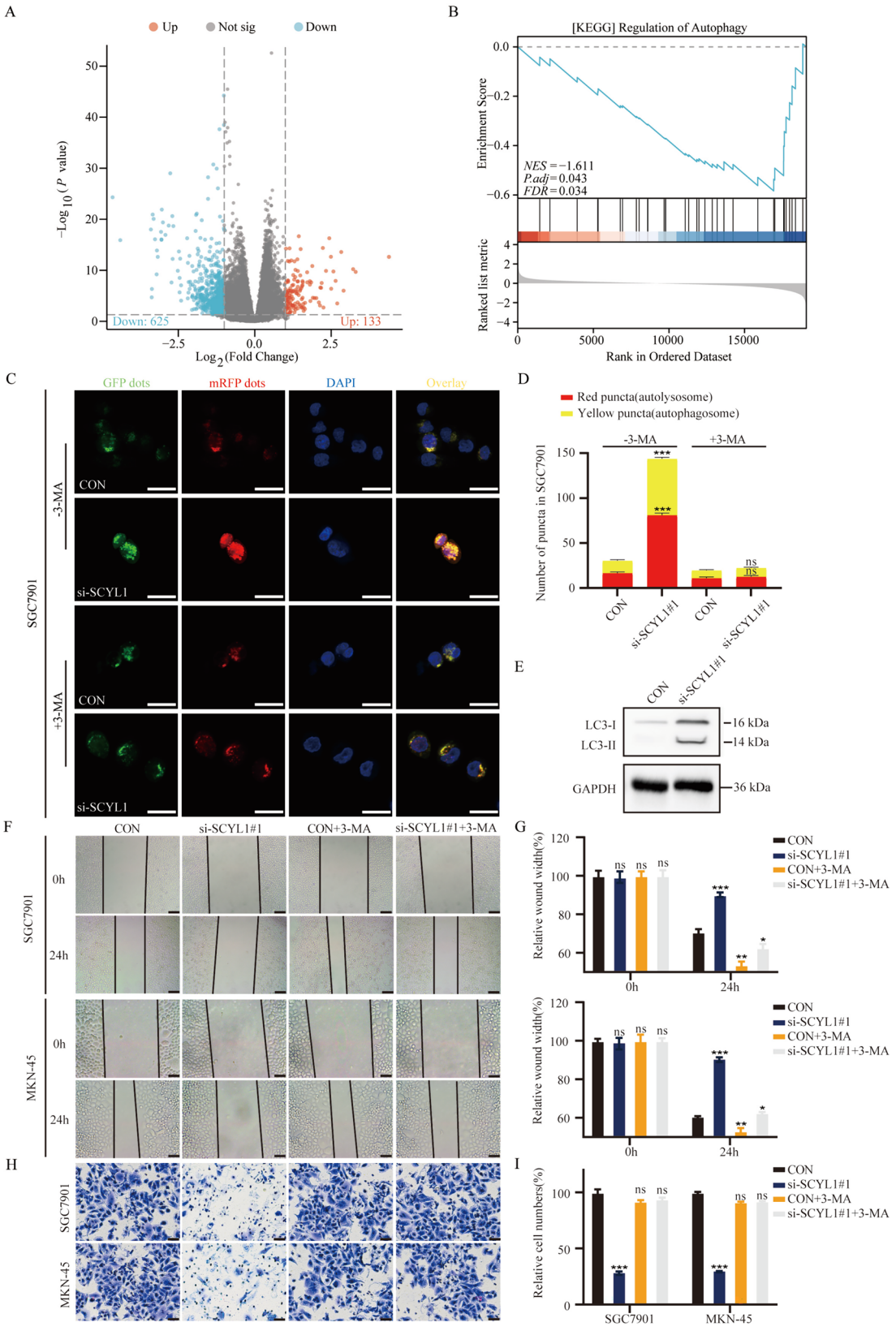
A
Up
Not sig
Down
−Log10(P value)
Log2(Fold Change)
Down: 625
Up: 133
B
[KEGG] Regulation of Autophagy
Enrichment Score
NES = −1.611
P.adj = 0.043
FDR = 0.034
Ranked list metric
Rank in Ordered Dataset
C
GFP dots
mRFP dots
DAPI
Overlay
SGC7901
-3-MA
+3-MA
CON
si-SCYL1
D
Red puncta(autolysosome)
Yellow puncta(autophagosome)
Number of puncta in SGC7901
E
LC3-I
LC3-II
GAPDH
16 kDa
14 kDa
36 kDa
F
CON
si-SCYL1#1
CON+3-MA
si-SCYL1#1+3-MA
0h
24h
MKN-45
G
Relative wound width(%)
H
I
Relative cell numbers(%)

◂**Fig. 4** SCYL1 inhibits autophagy in GC cells, promoting their migration and invasion. (**a**) Volcano plot based on high and low expression genes of SCYL1 in TCGA. (**b**) GSEA enrichment analysis sorted by log2FC values from high to low, based on the TCGA database. Gene set: "c2.cp.all.v2022.1.Hs.symbols.gmt". (**c**) Detection of autophagic flux using GFPmRFP-LC3 lentivirus in CON or si-SCYL1 SGC7901 groups. Scale bar, 20 μm. (**d**) Quantification of LC3 dots (red and yellow representing autophagosomes or autolysosomes, respectively) in CON or si-SCYL1 SGC7901 groups. (**e**) Western blot analysis of autophagy-related markers: LC3 and P62 protein levels, with GAPDH as an internal reference. (**f–i**) Transwell and wound healing assays to assess the effect of autophagy inhibitor 3-MA on restoring the migratory ability of GC cells treated with si-SCYL1. Scale bar, 50 μm. (ns, $P > 0.05$; *$P < 0.05$; **$P < 0.01$; ***$P < 0.001$)

the mTORC1 signaling pathway. Therefore, future research might explore inhibitors or antagonists of SCYL1 as new directions for GC treatment. Moreover, our study suggests that the expression level of SCYL1 could serve as a valuable biomarker for the prognosis of GC in clinical settings.

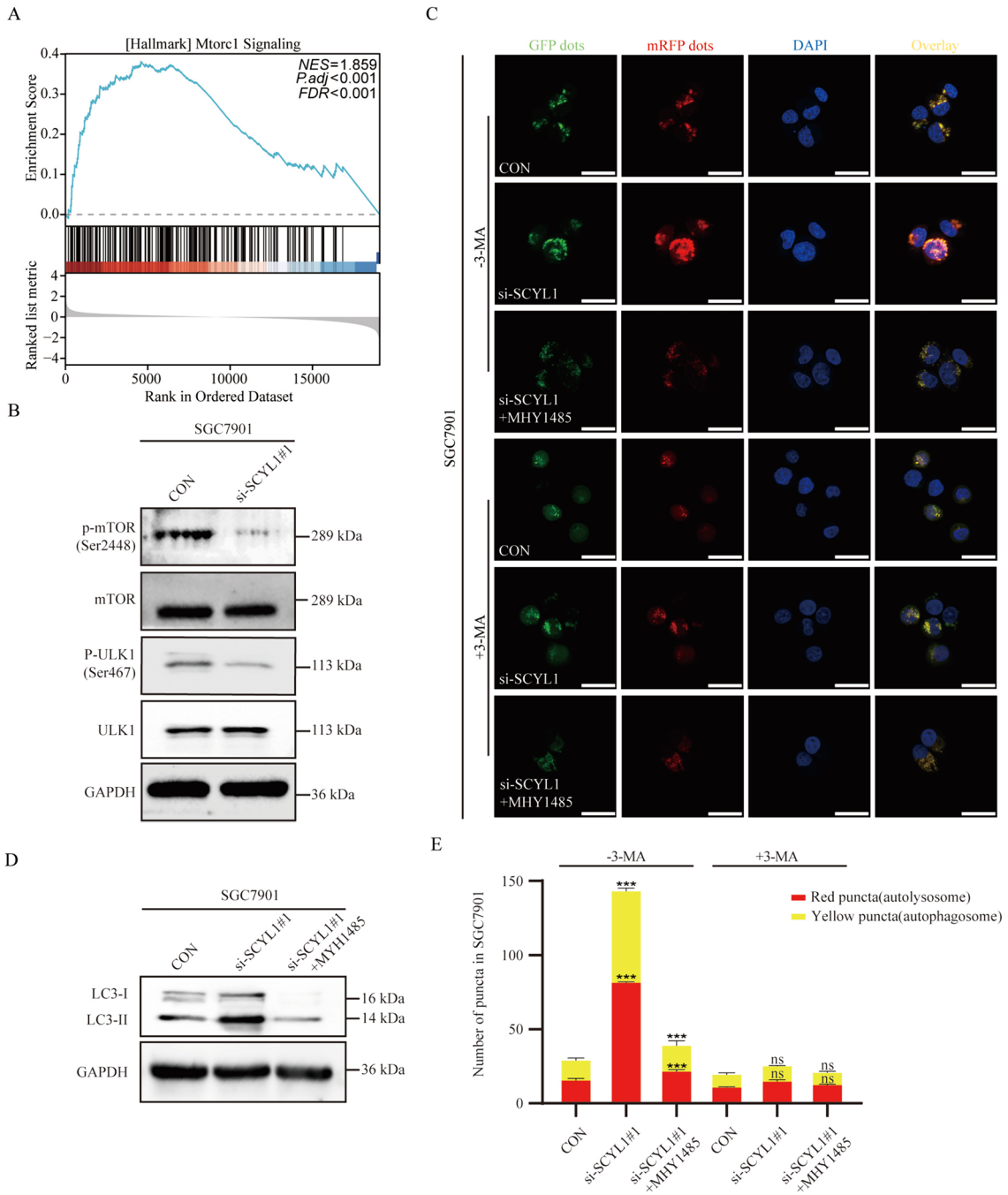

Fig. 5 SCYL1 inhibits autophagy in GC cells by activating the mTORC1 signaling pathway. (**a**) Gene Set Enrichment Analysis (GSEA) based on the TCGA database, sorted by log2FC values from high to low. The gene set used is "h.all.v7.5.1.symbols.gmt". (**b**) WB analysis to detect the levels of proteins related to the mTORC1 pathway. (**c**) WB analysis of the impact of si-SCYL#1 and the mTOR Agonist MHY1485 on autophagy levels in SGC-7901. (**d**) Detection of autophagic flux using the GFPmRFP-LC3 lentivirus in CON, si-SCYL1, and si-SCYL1 + MHY14845 SGC7901 groups. Scale bar, 20 μm. E. Quantification of LC3 in CON, si-SCYL1, and siSCYL1 + MHY14845 SGC7901 groups (red and yellow represent autophagosomes or autolysosomes, respectively). (ns, $P > 0.05$; ***$P < 0.001$)

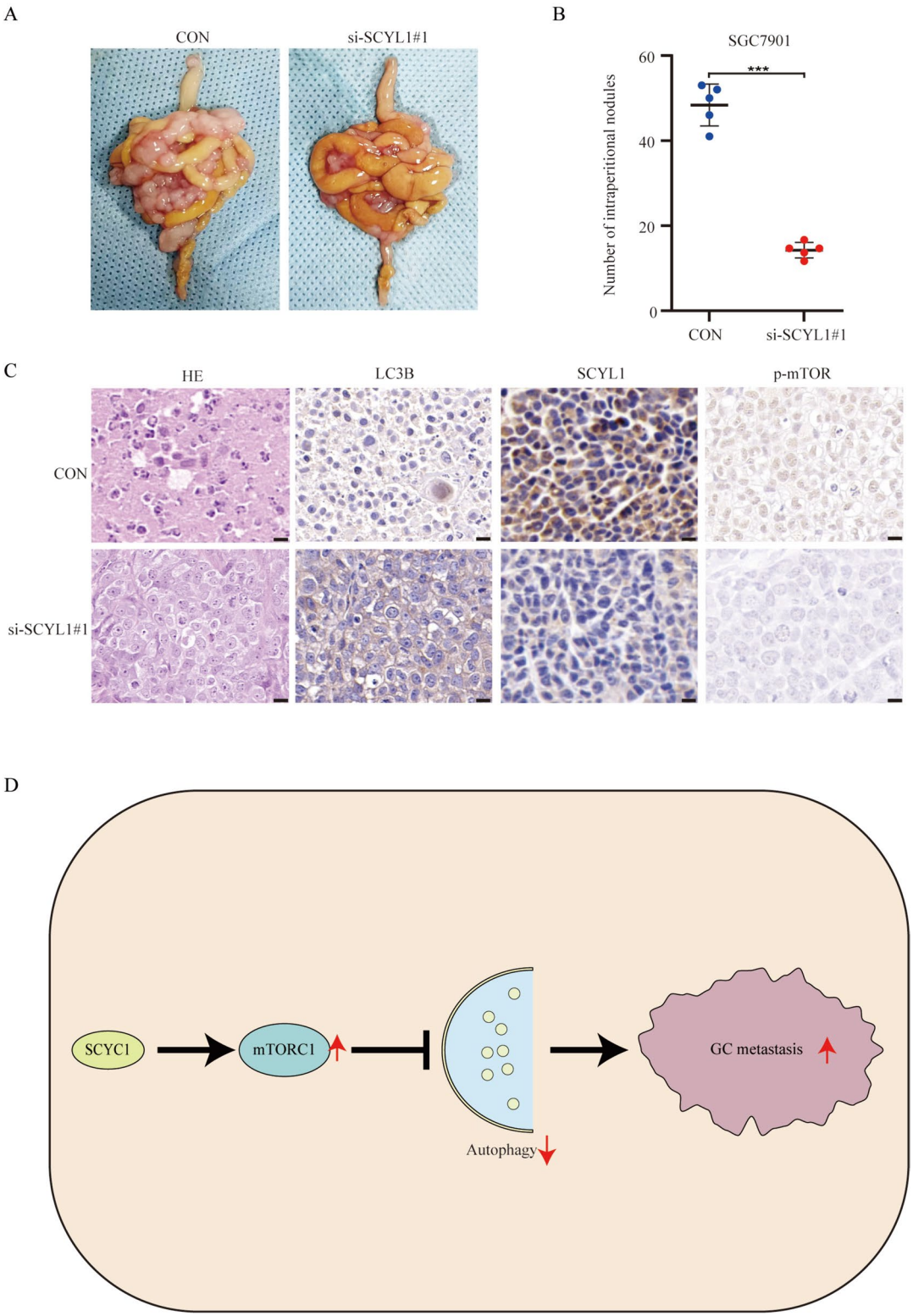

Fig. 6 SCYL1 promotes the migration of GC in vivo. (**a**, **b**) Representative images and numbers of intraperitoneal metastatic nodules in nude mice injected with recombinant GC cells and control cells. (**c**) HE and IHC staining intensity for SCYL1, LC3B, and p-mTOR in different groups. Scale bar, 10 μm. (**d**) Summary of the findings: SCYL1 promotes GC migration by activating the mTORC1 signaling pathway and inhibiting autophagy in GC cells

Acknowledgements We thank the patients and their families and all colleagues who contributed in this study.

Author contributions Wanjiang Xue and Weijie Zang contributed to the conception and design of the study. Yilin Hu, Junjie Chen and Jinlong Liu performed the bioinformatics analysis and prepared the manuscript. Zihao Zhao, Zhuzheng Chen and Xian Gao were responsible for the specific experimental operations and data analysis.

Funding This work was supported by the National Natural Science Foundation of China (82102720), Natural Science Foundation of Nantong (JC2023092), Natural Science Foundation of the Jiangsu Province, China (BK20221272), Fundation of Jiangsu Province Research Hospital (YJXYY202204-ZD18), Science and Technology Bureau of Nantong (JC12022107) and Postgraduate Research and Practice Innovation Program of Jiangsu Province (KYCX24_3580 and SJCX24_2055).

Data availability The data that support the findings of this study are available on request from the corresponding author.

Declarations

Conflict of interest The authors declare that the research was conducted in the absence of any commercial or financial relationships that could be construed as a potential conflict of interest.

Ethics statement Written informed consent was obtained from all patients and all procedures were approved by the Institutional Research Ethics Committee (2023-K076-01).

References

Aslan C, Maralbashi S, Salari F, Kahroba H, Sigaroodi F, Kazemi T et al (2019) Tumor-derived exosomes: Implication in angiogenesis and antiangiogenesis cancer therapy. J Cell Physiol 234(10):16885–16903

Chen Y, Wang B, Zhao Z, Li M, Wang F (2022) PRSS2 overexpression relates to poor prognosis and promotes proliferation, migration and invasion in gastric cancer. Tissue Cell 79:101949

Chen K, Yu B, Liao J (2021) LncRNA SOX2OT alleviates mesangial cell proliferation and fibrosis in diabetic nephropathy via Akt/mTOR-mediated autophagy. Mol Med 27(1):71.

Debnath J, Gammoh N, Ryan KM (2023) Autophagy and autophagy-related pathways in cancer. Nat Rev Mol Cell Biol 24(8):560–575

Hao Y, Hao S, Andersen-Nissen E, Mauck WM, 3rd, Zheng S, Butler A, et al. (2021) Integrated analysis of multimodal single-cell data. Cell 184(13):3573–3587 e29.

Hou J, Han Z, Zhao N, Wei L (2020) Autophagy and tumour metastasis. Adv Exp Med Biol 1207: 315–338.

Hu L, Liu M, Chen L, Chan THM, Wang J, Huo K-k, Zheng B-J, Xie D, Guan X-Y (2012) SCYL1 binding protein 1 promotes the ubiquitin-dependent degradation of Pirh2 and has tumor-suppressive function in the development of hepatocellular carcinoma. Carcinogenesis 33(8):1581–1588. https://doi.org/10.1093/carcin/bgs162

Hu Y, Chen Y, Wu M, Qian C, Chen J, Wang K et al (2024) Integrin-based prognostic model predicts survival, immunotherapy response, and drug sensitivity in gastric cancer. Biomed Technol 5:26–45

Jiang H, Dingyi Y, Yang P, Guo R, Kong M, Gao Y, Xiongfei Y, Xiaoyan L, Fan X (2022) Revealing the transcriptional heterogeneity of organ-specific metastasis in human gastric cancer using single-cell RNA Sequencing. Clin Translat Med 12(2):e730. https://doi.org/10.1002/ctm2.730

Karlin KL, Mondal G, Hartman JK, Tyagi S, Kurley SJ, Bland CS et al (2014) The oncogenic STP axis promotes triple-negative breast cancer via degradation of the REST tumor suppressor. Cell Rep 9(4):1318–1332

Ke S, Li RC, Lu J, Meng FK, Feng YK, Fang MH (2017) MicroRNA-192 regulates cell proliferation and cell cycle transition in acute myeloid leukemia via interaction with CCNT2. Int J Hematol 106(2):258–265

Kuliyev E, Gingras S, Guy CS, Howell S, Vogel P, Pelletier S (2018) Overlapping role of SCYL1 and SCYL3 in maintaining motor neuron viability. J Neurosci 38(10):2615–2630

Lei MML, Leung CON, Lau EYT, Leung RWH, Ma VWS, Tong M, Yin Ying L, Huang CY, Zhu QH, Ng IOL, Ma S, Lee TKW (2023) SCYL3, as a novel binding partner and regulator of ROCK2, promotes hepatocellular carcinoma progression. JHEP Rep 5(1):100604. https://doi.org/10.1016/j.jhepr.2022.100604

Li S, Sheng J, Liu Z, Fan Y, Zhang C, Lv T et al (2021) Potent antitumour of the mTORC1/2 dual inhibitor AZD2014 in docetaxel-sensitive and docetaxel-resistant castration-resistant prostate cancer cells. J Cell Mol Med 25(5):2436–2449

Liu D, Wang W, Zeng Z, Liu X, Zhou Y, Wang C et al (2023) Elevated pretreatment squamous cell Carcinoma Antigen indicates unfavorable treatment outcomes in cervical cancer patients receiving definitive radiotherapy. Precis Radiat Oncol 7(3):173–180

Liu J-Z, Hu Y-L, Feng Y, Jiang Y, Guo Y-B, Liu Y-F, et al. (2020) BDH2 triggers ROS-induced cell death and autophagy by promoting Nrf2 ubiquitination in gastric cancer. J Exp Clin Cancer Res 39(1): 123.

Marsh T, Debnath J (2020) Autophagy suppresses breast cancer metastasis by degrading NBR1. Autophagy 16(6):1164–1165

Maynard A, McCoach CE, Rotow JK, Harris L, Haderk F, Kerr DL et al (2020) Therapy-induced evolution of human lung cancer revealed by single-cell RNA sequencing. Cell 182(5):1232-1251. e22

Pelletier S (2016) SCYL pseudokinases in neuronal function and survival. Neural Regen Res 11(1):42. https://doi.org/10.4103/1673-5374.175040

Saxton RA, Sabatini DM (2017) mTOR signaling in growth, metabolism, and disease. Cell 168(6):960–976

Subramanian A, Tamayo P, Mootha VK, Mukherjee S, Ebert BL, Gillette MA, Paulovich A, Pomeroy SL, Golub TR, Lander ES, Mesirov JP (2005) Gene set enrichment analysis: A knowledge-based approach for interpreting genome-wide expression profiles. Proc Natl Acad Sci 102(43):15545–15550. https://doi.org/10.1073/pnas.0506580102

Sun A, Tian X, Yang W, Lin Q (2022) Overexpression of SCYL1 is associated with progression of breast cancer. Curr Oncol 29(10):6922–6932

Sung H, Ferlay J, Siegel RL, Laversanne M, Soerjomataram I, Jemal A, Bray F (2021) Global Cancer Statistics 2020: GLOBOCAN Estimates of Incidence and Mortality Worldwide for 36 Cancers in 185 Countries. CA A Cancer J Clinicians 71(3):209–249. https://doi.org/10.3322/caac.21660

Tang X, Ding H, Liang M, Chen X, Yan Y, Wan N et al (2021) Curcumin induces ferroptosis in non-small-cell lung cancer via activating autophagy. Thorac Cancer 12(8):1219–1230

Thrift AP, El-Serag HB (2020) Burden of gastric cancer. Clin Gastroenterol Hepatol 18(3):534–542

Yan J, Di Y, Shi H, Rao H, Huo K (2010) Overexpression of SCYL1-BP1 stabilizes functional p53 by suppressing MDM2-mediated ubiquitination. FEBS Lett 584(20):4319–4324

Yang H, Jiang X, Li B, Yang HJ, Miller M, Yang A et al (2017) Mechanisms of mTORC1 activation by RHEB and inhibition by PRAS40. Nature 552(7685):368–373

Zang WJ, Wang ZN, Hu YL, Huang H, Ma P (2021) Expression of fatty acid-binding protein-4 in gastrointestinal stromal tumors and its significance for prognosis. J Clin Lab Anal 35(11):e24017. https://doi.org/10.1002/jcla.24017

Zang WJ, Hu YL, Qian CY, Feng Y, Liu JZ, Yang JL et al (2022) HDAC4 promotes the growth and metastasis of gastric cancer via autophagic degradation of MEKK3. Br J Cancer 127(2):237–248